

Two photon versus one photon fluorescence excitation in whispering gallery mode microresonators.

Carme Pastells^{1,2}, M.-Pilar Marco^{1,2}, David Merino³, Pablo Loza-Alvarez³, Laura Pasquardini⁴, Lorenzo Lunelli^{4,5}, Cecilia Pederzoli⁴, Nicola Daldosso⁶, Daniele Farnesi^{7,8}, Simone Berneschi⁷, Giancarlo C. Righini^{7,8}, F. Quercioli⁹, Gualtiero Nunzi Conti⁷, Silvia Soria^{7*}

¹Nanobiotechnology for Diagnostics group (Nb4Dg), IQAC-CSIC, 08034-Barcelona, Spain

²CIBER de Bioingeniería, Biomateriales y Nanomedicina, 08034-Barcelona, Spain

³ICFO-Institut de Ciències Fotòniques, 08860-Castelldefels, Barcelona, Spain

⁴Fondazione Bruno Kessler, 38123 Povo (TN), Italy

⁵IBF-CNR, 38123 Povo (TN), Italy

⁵Department of Computer Science, University of Verona, Strada le Grazie 15, 37134 Verona, Italy

⁶CNR-IFAC “Nello Carrara” Institute of Applied Physics, 50019 Sesto Fiorentino (FI), Italy

⁷Museo Storico della Fisica e Centro Studi e Ricerche “E. Fermi”, 00184 Roma, Italy.

⁸CNR-INO National Institute of Optics, Sesto Fiorentino (Fi) Italy

*s.soria@ifac.cnr.it

ABSTRACT

We investigate the feasibility of both one photon and two photon fluorescence excitation using whispering gallery mode microresonators. We report the linear and non linear fluorescence real-time detection of labeled IgG covalently bonded to the surface of a silica whispering gallery mode resonator (WGMR). The immunoreagents have been immobilized onto the surface of the WGMR sensor after being activated with an epoxy silane and an orienting layer. The developed immunosensor presents great potential as a robust sensing device for fast and early detection of immunoreactions. We also investigate the potential of microbubbles as nonlinear enhancement platform. The dyes used in these studies are dylight800, tetramethyl rhodamine isothiocyanate, rhodamine 6G and fluorescein. All measurements were performed in a modified confocal microscope.

Keywords: whispering gallery modes resonators, microspheres, non- linear fluorescence

Two photon versus one photon fluorescence excitation in whispering gallery mode microresonators.

Carme Pastells^{1,2}, M.-Pilar Marco^{1,2}, David Merino³, Pablo Loza-Alvarez³, Laura Pasquardini⁴, Lorenzo Lunelli^{4,5}, Cecilia Pederzoli⁴, Nicola Daldosso⁶, Daniele Farnesi^{7,8}, Simone Berneschi⁷, Giancarlo C. Righini^{7,8}, F. Quercioli⁹, Gualtiero Nunzi Conti⁷, Silvia Soria^{7*}

¹Nanobiotechnology for Diagnostics group (Nb4Dg), IQAC-CSIC, 08034-Barcelona, Spain

²CIBER de Bioingeniería, Biomateriales y Nanomedicina, 08034-Barcelona, Spain

³ICFO-Institut de Ciències Fotòniques, 08860-Castelldefels, Barcelona, Spain

⁴Fondazione Bruno Kessler, 38123 Povo (TN), Italy

⁵IBF-CNR, 38123 Povo (TN), Italy

⁶Department of Computer Science, University of Verona, Strada le Grazie 15, 37134 Verona, Italy

⁷CNR-IFAC “Nello Carrara” Institute of Applied Physics, 50019 Sesto Fiorentino (FI), Italy

⁸Museo Storico della Fisica e Centro Studi e Ricerche “E. Fermi”, 00184 Roma, Italy.

⁹CNR-INO National Institute of Optics, Sesto Fiorentino (Fi) Italy

*s.soria@ifac.cnr.it

ABSTRACT

We investigate the feasibility of both one photon and two photon fluorescence excitation using whispering gallery mode microresonators. We report the linear and non linear fluorescence real-time detection of labeled IgG covalently bonded to the surface of a silica whispering gallery mode resonator (WGMR). The immunoreagents have been immobilized onto the surface of the WGMR sensor after being activated with an epoxy silane and an orienting layer. The developed immunosensor presents great potential as a robust sensing device for fast and early detection of immunoreactions. We also investigate the potential of microbubbles as nonlinear enhancement platform. The dyes used in these studies are dylight800, tetramethyl rhodamine isothiocyanate, rhodamine 6G and fluorescein. All measurements were performed in a modified confocal microscope.

Keywords: whispering gallery modes resonators, microspheres, non- linear fluorescence

1. INTRODUCTION

Whispering gallery mode resonators (WGMR) are evanescent wave sensors that can be used both as refractometres or label-free sensors and fluorescence based sensors [1, 2]. The disadvantages of the labeled system—namely, cost and possibly reduced reactivity—are normally compensated by lower limit of detection (LOD), while in the case of direct monitoring, the limitations lie in the ineffectiveness of detecting small

1
2
3
4 molecular weight analytes and in the sensitivity to non-specific binding. In a WGMR light is trapped by total
5 internal reflection at the resonator interface and the evanescent tail of the electromagnetic field interacts with
6 the analytes on the resonator surface. WGMR can achieve very high quality factors Q [3] which means high
7 sensitivity. A crucial step for producing reliable biosensors is the surface functionalization, or chemical
8 modification of the transducer surface in order to bind the biological recognition element on it. This
9 functional layer has to be very thin, between 10-100 nm and homogeneous, in order to preserve the high
10 quality of the transducer and the interaction with the sensing layer and the WGMR [4, 5]. The permanence of
11 high Q values after the functionalization of the surface is an essential requirement in order to achieve highly
12 sensitive devices.
13

14
15
16 For that reason, most of the efforts have been directed to label-free detection, even though the feasibility of
17 using WGMR as platforms for one photon fluorescence (OPF) detection has been studied [6]. Based on these
18 recent papers, we tested first the feasibility of OPF with spherical WGMR where antibodies against
19 *Staphylococcus aureus* cell wall labeled with a near infrared dye (Dylight800, Thermo Scientific) were
20 immobilized on its surface. *S. aureus* is a bacterium that can cause a range of illnesses, from minor skin
21 infections to life threatening diseases. Moreover, this pathogen is one of the five most common causes of
22 nosocomial infections.
23

24
25 It is true that commercial NIR dyes are excellent but their intrinsically small Stokes shift may produce
26 excitation and scattered light interferences, especially when the excitation light used is a tunable diode laser.
27 The wide gain profile of the semiconductor easily masks the emitted fluorescence due to the overlap with the
28 emission spectrum of the dye [7]. Being that our case, we decided to resort to a nonlinear detection technique
29 like two photon fluorescence (TPF), which was already validated as a very good detection technique for
30 labeled peptides [8] and steroids [9,10]
31

32
33 As mentioned above, TPF measurements with near infra-red radiation have a number of advantages over
34 measurements with OPF. Specifically, the large energy gap between the excitation and emission radiation
35 reduces the background noise, the static photobleaching of the dyes that are used is reduced because there is a
36 quadratic dependence of the absorption on intensity [11,12], and the use of near infra-red radiation (NIR)
37 minimizes the photodamage of cells and tissue thereby lowering autofluorescence. On the other hand,
38 conventional TPF requires highly intense and focused laser light of instantaneous photon flux densities of at
39 least 10^{31} photons/cm², which in turn lowers the photodamage threshold [13]. In order to overcome such a
40 difficulty, i.e. to achieve the needed energies and yet avoid tight focusing, we resort to low-loss, high-quality
41 factor whispering gallery mode resonators (WGMR) [1,14]. Another reason to use TPF is the available wide
42 range of visible fluorescent dyes with very high quantum yields and molar extinction coefficients.
43

44
45 The TPF measurements were performed in a modified confocal microscope; we coupled the excitation light
46 with a 4X and 10X objective and detected the TPF signal with a CCD camera. We performed all
47 measurements with a femtosecond laser (Ti:Sapphire, Coherent) in order to avoid secondary effects in the
48 biological layers or in the organic solutions. We report the observation of TPF, first in microbubbles WGMR
49 filled with a 10^{-3} M and 10^{-4} M solution of fluorescein and then 10^{-6} M solution of Rhodamine 6G, in the latter
50 the concentration is three orders of magnitude lower than previous work [14]; and in microspheres coated
51 with labeled IgG.
52
53

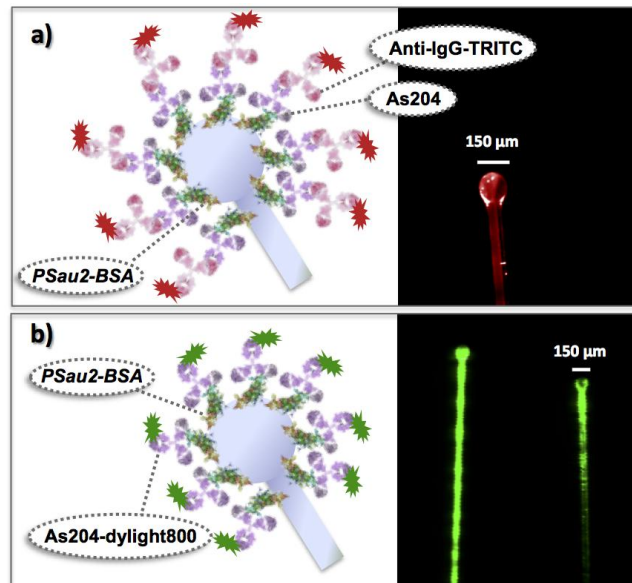
54 55 **2. EXPERIMENTAL RESULTS AND DISCUSSION.**

56 57 **2.1 Surface functionalization Method.**

58
59
60
61
62
63
64
65

1
2
3
4 The microspheres were functionalized following three different procedures. The first batch of microspheres
5 were functionalized as follows: before exposing to the epoxy silanes, microspheres were soaked into piranha
6 solution ($H_2SO_4:H_2O$ (7:3)) for 3 min minutes to remove organic contaminants and oxidize the surface, then
7 rinsed in MilliQ water, soaked in 10% NaOH (w/v) for 1 h, washed again in milliQ water and absolute EtOH.
8 The activated spheres were then soaked in 98% (3-glycidyloxypropyl)-trimethoxysilane (GPTMS) for 1h,
9 dried in air and stored under vacuum. The epoxy-derivatized microspheres were coated with PSau2-BSA
10 (0.125 $\mu\text{g/mL}$ in printing buffer -150 mM sodium phosphate buffer, 0.001% sodium dodecyl sulfate, pH 8.5)
11 3 h at room temperature (RT). Then, the microspheres were washed with PBST (10 mM phosphate buffer on a
12 140 mM NaCl solution with 0.05% Tween 20, pH 7.5) and the specific antibody (As204, 0.02 mg/mL in
13 PBST) was added for 30 min at RT. After another cycle of wash with PBST, the microspheres were labelled
14 with commercially anti-IgG conjugated to tetramethyl rhodamine isothiocyanate (TRITC) (0.02 mg/mL in
15 PBST). Then, the microspheres were washed with PBST and MilliQ water and the fluorescent derivatization
16 of the microspheres was verified. The uniformity and fluorescence emission of the IgG-TRITC was checked
17 in a commercial confocal microscope (OPF) (figure 1.a)

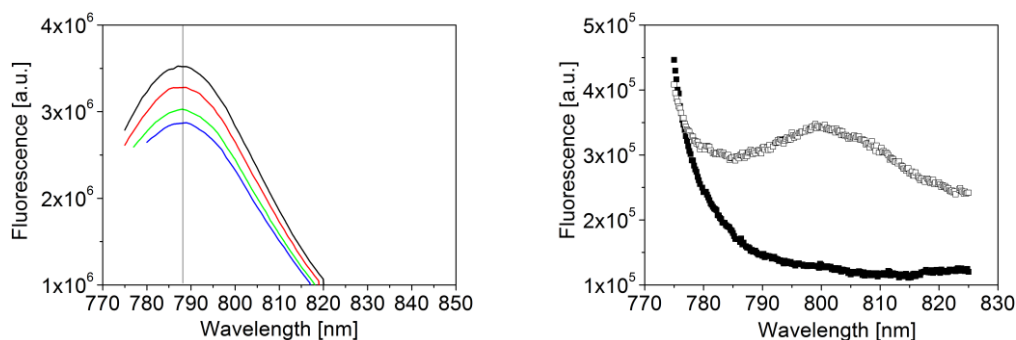
18
19
20
21
22 The second batch of microspheres were functionalized and coated with PSau2-BSA following the same
23 procedure described for the first batch. Then, the microspheres were washed with PBST and the specific
24 antibody labeled with the dylight800 fluorophore (As204-dylight800, 0.02 mg/mL in printing buffer) was
25 added for 30 min at RT. The As204-dylight800 conjugate was prepared in one of our labs, three different
26 molar ratios of As204:dylight800 were tested: 1:1; 1:2 and 1:10). After, the microspheres where washed
27 with PBST and finally with MilliQ water. In order to verify the fluorescent derivatization of the microspheres,
28 we checked the uniformity and fluorescence emission of the As204-dylight800 with a LICOR Odyssey scanner
29 Figure 1.b. shows the ratio 1:2 as an example, since all molar ratios were uniform and gave good signal.
30
31
32
33
34
35



57
58 Fig. 1. a) Microsphere labelled with Anti-IgG-TRITC (fluorescence 2.5X) and b) microsphere labelled with As204-
59 dylight800 (molar ratio 1:2).
60
61
62
63
64
65

1
2
3
4
5 The third batch of microspheres was functionalized as follows: after oxidizing the surface with the piranha
6 solution, (H_2SO_4 : H_2O_2 (4:1 v/v) for 3 min), the spheres were immersed in a 0,01% solution of 3-
7 glycidoxypropyl-trimethoxysilane (GPTMS) in anhydrous toluene at 60° C for 1 min. On this second batch, in
8 order to avoid random orientation of the antibodies we immobilized covalently an orienting layer of protein G
9 (10 mg/ml in phosphate buffer 100 mM pH 8 for 2 hours) that binds antibodies with a high affinity through
10 the Fc region, leaving the Fab sites free for interaction. Then we bound: a) As204 conjugated with dylight800
11 (1:2 and 1:10) and b) IgG labelled with tetramethyl rhodamine isothiocyanate (TRITC) both at 8 $\mu\text{g}/\mu\text{l}$ ml in
12 phosphate buffer 100 mM pH 8 at room temperature for two hours.

13
14
15 Dylight 800 is a fluorescent dye with a maximum absorption at 777 nm and a maximum emission at 794 nm
16 (Pierce, datasheet). However, the physical characteristics of fluorescent dyes change depending on the
17 surroundings (emission and excitation wavelengths and also lifetime). This is especially true when dyes are
18 covalently bound to biomolecules and dried monolayers. We checked the fluorescence emission of a solution
19 of As204-dylight800 (molar ratio 1:10) in phosphate buffer (100 mM, pH 8) for four different excitation
20 wavelengths (770, 772, 775 and 777 nm) using a FluoroMax®-4 Fluorescence Spectrophotometer (HORIBA
21 Scientific). As it can be seen in figure 2.a., the maximum emission occurs at 788 nm independently on the
22 excitation wavelength (between 770 and 777 nm) whereas the maximum excitation wavelength is 770 nm.
23 Figure 2.b. shows the emission spectra of a mock microsphere (silica glass slide functionalised with and
24 without a covalently bound layer of As204-dylight800), analyzed by using the Fluorescence Spectrometer.
25 The maximum emission is shifted towards longer wavelength of about 13 nm with respect to the dylight800
26 conjugated As204 solution, as expected [7].
27
28
29
30
31
32



46 Fig. 2. a) Emission spectra of a dylight800 conjugated As204 solution for different excitation wavelengths (black:
47 770nm; red: 772 nm; green: 775 nm and blue: 777nm); b) Emission spectra of a mock microsphere in two different
48 conditions: empty squares: silica glass slide mimicking the 3rd batch of microspheres; filled squares: functionalized
49 silica glass slide without the bioconjugate As204-dylight800.
50
51
52
53

54 2.2 One photon fluorescence measurements.

55
56
57
58
59
60
61
62
63
64
65

1
2
3
4 The experimental setup for measuring the quality factor and OPF is sketched in Fig.3. The light from a fiber pigtailed tunable diode laser (TDL) is tunable from 765 nm to 781 nm. A polarization controller and a tap coupler (5%, not shown in Fig. 3) allow adjusting the polarization state and monitoring the lunched pump power. Light is then coupled to the WGMR by means of a fiber taper, also produced in-house. The laser is tuned into a resonance from high to low frequencies, which results in thermal self-locking [15] of the WGMR mode to the pump laser. Fluorescence was detected on an optical spectrum analyzer (OSA) or a spectrometer by collecting with a multimode fiber (MMF, 50 μm core, 0.2 NA) the light scattered from the microsphere using a long pass filter (RG780, Schott). A 3dB splitter at the fiber output (not shown in Fig. 3) has one end on the spectrometer and the other on a detector connected to an oscilloscope, which allows locating the resonance positions while scanning the laser.

17 Silica microspheres can be easily fabricated directly on the tip of a standard telecom fiber using a sequence of arc discharges of a fiber fusion splicer [16]. We fabricated spheres of different diameters, ranging from about 125 μm to 180 μm . The residual fiber stem is then mounted on a translation stage with piezoelectric actuators and a positioning resolution of 20 nm.

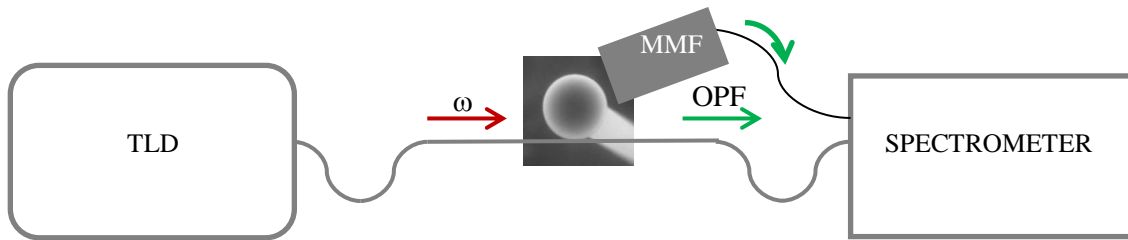
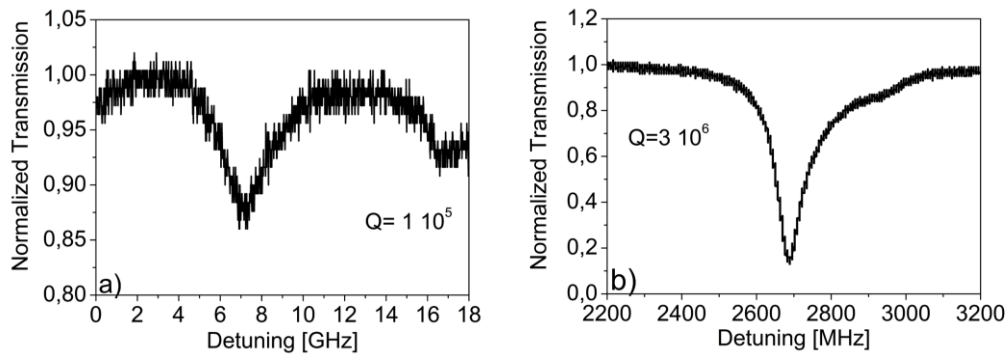


Fig. 3. Scheme of the experimental setup. TLD: Tunable laser diode; MMF: multimode fiber, OPF: one photon fluorescence.

39 We measured the quality factor of the functionalized microspheres at two wavelengths: at 1550 nm (without absorption) and at 770 nm (maximum absorption). The quality factor at 1550 nm of the first and second batch of microspheres were in excess of 10^6 whereas for the third one the quality factor was in excess of 10^7 (not shown in here). At 770 nm, due to the absorption of the dye, the Q factor lowered by one order of magnitude for both functionalized microspheres (figure 4).



1
2
3
4
5
6
7
8
9
10
11
12
13
14
15
16
17
18
19
20
21
22
23
24
25
26
27
28
29
30
31
32
33
34
35
36
37
38
39
40
41
42
43
44
45
46
47
48
49
50
51
52
53
54
55
56
57
58
59
60
61
62
63
64
65

Figure 4. Q factor at 770 nm of the microspheres with 1:2 ratio As204-dylight800 covalently bound to the surface: a) first batch and b) third batch.

In principle, the evanescent tail of the WGM should be overlapping with the biological layer and interacting with the As204-Dylight800. With this idea in mind, we proceeded to measure the scattered OPF with a MMF connected to a hand held spectrometer. Figure 5.a. and 5.b. show the collected scattered light for a microsphere of at diameter of about 180 μm and the laser emission spectrum, respectively. In figure 5.a the excitation wavelength was centered at 770 nm and the power of the laser was attenuated from 148 μW down to 245 nW. All microsphere batches show similar behavior.

Despite of how promising the graphs look, there is a main discrepancy between the emitted OPF from the surface of the microsphere and the OPF measured with a commercial scanner: the emission peak was expected at 814nm for a dry environment (fig.2.b) and in the graphs it is at 780 nm. The center wavelength of the TLD is at 770 nm with an output power (1 mW) but the gain bandwidth of the laser is extended from 760 to 790 nm and at 780 nm the power is about 0.1 μW with a shape that resembles too much the spectra shown in fig.5.a. without the convolution of the filter (see fig.5.b).

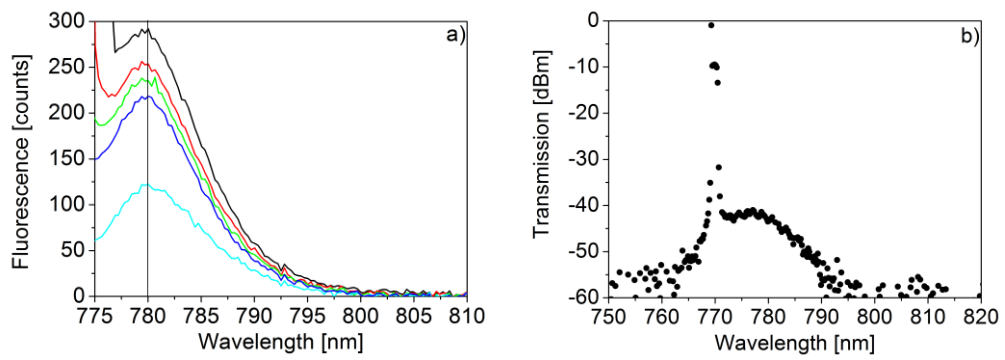


Fig. 5. a) Scattered light measured with a hand held spectrometer from the second batch of microspheres with As204-Dylight800 1:2 ratio As204-Dylight800 covalently bound to the surface microsphere of a diameter of about 140 μm (black 148 mW, red 92 mW, gree 42 mW, blue 2 mW, cyan 398 nW); b) Laser spectrum measured with an OSA.

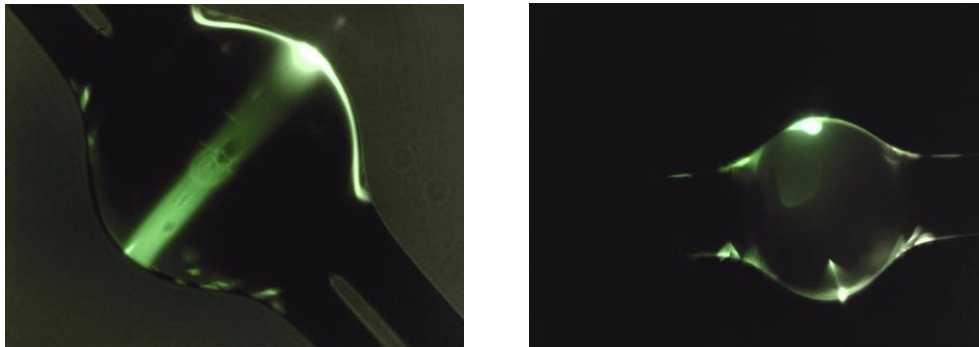
In order to discriminate whether the scatter light we measured is OPF or mainly the scattered excitation laser light, we tuned the excitation wavelength to the red edge of the bandwidth of the laser, namely, 788 nm. At this wavelength, there is no excitation light that can heavily interfere with the OPF of the dye. We didn't observe OPF, not even for larger integration times and more averaged signal. We concluded that the measured scattered signal is just the excitation laser scattered by the microsphere and convoluted by the filter. For that

1
2
3
4 reason we resorted to TPE of microspheres covalently bound IgG labeled with TRITC ($8 \mu\text{g}/\mu\text{l}$ in 100 mM
5 phosphate buffer, pH 8).
6

7 **2.3 Two photon excitation in microbubbles and microspheres.**

8
9 The MBRs were fabricated from slightly pressurized silica capillaries using a modified fusion splicer, where
10 the electrodes could rotate by 360° by means of a step by step motor. Details of the fabrication can be found
11 in our previous work [17]. Reproducibility is ensured by the control of all physical parameters of the process
12 (duration and power of arc discharges, gas pressure, rotation speed, distance between capillary and
13 electrodes). The microbubbles were the filled with a 10^{-3}M and 10^{-4} M solution of fluorescein and 10^{-6} M
14 solution of Rhodamine 6G.
15
16

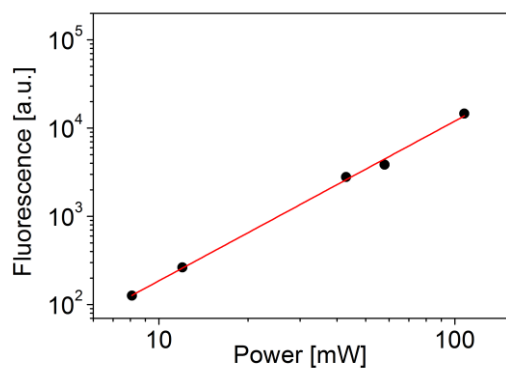
17 We used a modified confocal microscope for coupling the light into the microbubble resonator [18]. We used
18 an inverted light microscope (Nikon Eclipse TE2000U). It can be used as a bright-field microscope or as a
19 phase contrast microscope. However its extendible design and advanced features make it ideal for upgrading
20 it to a multi-modal imaging system. The objectives that we used for this experiment was a 4X and 10X-
21 0.5NA dry objective. Due to the impressive average power capability, broad tuning range and short pulse
22 duration we used a commercial diode pumped, mode locked Ti: Sapphire laser (Coherent-MIRA 900f) for
23 our microscope. It has an average power of 1.2W, producing femtosecond pulses (150 fs) at a repetition rate
24 of 76 MHz. This instrument is tunable over a wavelength range of 690-950nm within which falls the two-
25 photon absorption spectra of many fluorophores [19]. The wavelength in the experiments was set to 800nm.
26 We set the voltage of the galvanometric mirrors to 0 in order to stop the raster scan of the beam and excite the
27 WGM of the microbubble by focusing the laser beam tangential to the bubble wall. The excitation light was
28 filtered by a dichoric mirror (FF720-SDi01, Semrock) and a BG39 Schott filter. We tested first the bubble
29 with the fluorescein filling that was imaged with a 4X dry objective using a CCD camera in order to see the
30 complete WGM at the equator. Figure 6.a. shows the TPF band around the equator and the TPF partially
31 coupled back to the MBR wall. The two lobes that correspond to the WGM are clearly seen (fig.6.b)
32
33
34
35
36
37
38
39



51
52
53 Fig.6. Fluorescence image of two different microbubbles, one filled with 10^{-3}M (a) and 10^{-4} M (b) fluorescein solution,
54 showing the TPF band. The image was taken with a 4X dry objective. The TPF coupled back to the MBR wall can be
55 also seen.
56
57
58
59
60
61
62
63
64
65

1
2
3
4
5
6
7
8
9
10
11
12
13
14
15
16
17
18
19
20
21
22
23
24
25
26
27
28
29
30
31
32
33
34
35
36
37
38
39
40
41
42
43
44
45
46
47
48
49
50
51
52
53
54
55
56
57
58
59
60
61
62
63
64
65

The two-photon nature of the emitted signal was validated by checking its dependence on the excitation laser power. Figure 7 shows a logarithmic representation of the TPEF signal from a Rhodamine 6G filled microbubble versus incident laser power at the focal plane. A linear fit to the data has slope 1.8 ± 0.1 ,



ensuring the quadratic dependence of the obtained signal.

Figure 7. Logarithmic presentation of the TPEF signal from the MBR filled with 10^{-6} M Rhodamine 6G solution versus incident laser power in log-log scale. The red line is the linear fit with slope close to 2.

After these results, we tested a microsphere where a layer of IgG labeled with TRITC was bound to its surface. Figure 8 shows the optical image of the microsphere where the coupling point and a partial WGM can be seen.

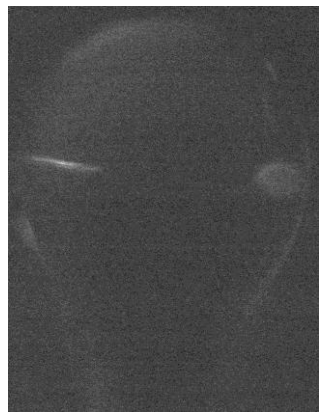


Figure 8. TPF image of the WGM excited in a microsphere, the coupling point and a partial WGM.

3. CONCLUSION

We have demonstrated the potential of microbubbles as nonlinear enhancement platform and verified the feasibility of exciting TPF via WGM in microspheres where labeled IgGs were covalently bound to its surface. The functionalization

1
2
3
4 process proved to be uniform, maintaining a good quality factor of the microresonators. In contrast to previous reports of
5 one photon fluorescence, we have demonstrated the impossibility of distinguish OPF from the excitation laser using
6 WGMR.
7
8
9

10 4. ACKNOWLEDGEMENTS

11 S. Soria acknowledges CNR funding from the STM 2014 program. CNR-IFAC and IQAC-CSIC teams acknowledge
12 funding from the CSIC-CNR bilateral projects. Funding from Centro Fermi is gratefully acknowledged. Funding from
13 Progetto Premiale CNR (2013-2015) is acknowledged. D. Farnesi is a PhD student at the University of Parma. F. Baldini
14 and A. Giannetti are gratefully acknowledged for their support and discussions.
15
16
17

18 REFERENCES

- 19
20
21 [1] S. Soria, S. Berneschi, M. Brenci, F. Cosi, G. Nunzi Conti, S. Pelli and G.C. Righini, Optical
22 microspherical resonators for biomedical applications, *Sensors* 11 (2011) 785.
23 [2] F. Vollmer, S. Arnold, Whispering-gallery-mode biosensing: label-free detection down to single
24 molecules, *Nat. Methods* 5 (2008) 591-596
25 [3] M. L. Gorodetsky, A. A. Savchenkov, V. S. Ilchenko, Ultimate Q of optical microspherical
26 resonators, *Opt. Lett.* 21 (1996) 453-455
27 [4] J. L. Nadeau, V. S. Ilchenko, D. Kossakovski, G. H. Bearman and L. Maleki, High-Q whispering-
28 gallery mode sensor in liquids, *Proceedings of SPIE* 4629 (2002) 172-180.
29 [5] S. Soria, F. Baldini, S. Berneschi, F. Cosi, A. Giannetti, G. Nunzi Conti, S. Pelli, G.C. Righini, B.
30 Tiribilli, High-Q polymer-coated microspheres for immunosensing applications. *Opt. Express* 17 (2009)
31 14694-14699.
32 [6] L. M. Freeman, S. Li, Y. Dayani, H-S. Choi, N. Malmstadt, A. M. Armani, Excitation of Cy5 in self-
33 assembled lipid bilayers using optical resonators, *Appl. Phys. Lett.* 98 (2011)143703
34 [7] C. Pastells, M. P. Marco, D. Merino, P. Loza-Alvarez, L. Pasquardini, C. Pederzoli, d. Farnesi, S.
35 Berneschi, G. C. Righini, G. Nunzi Conti, S. Soria, Nonlinear fluorescence excitation of Rhodamine 6G and
36 TRITC labeled IgG in whispering gallery mode microresonators, *Proc. SPIE* 9343 (2015)
37 doi:10.1117/12.2079112
38 [8] André Selle, Christoph Kappel, Mark Andreas Bader, Gerd Marowsky, Kathrin Winkler, and Ulrike
39 Alexiev, Picosecond pulse induced two photon fluorescence enhancement in biological material by
40 application of grating waveguide structures, *Opt. Lett* 30 (2005) 1683-1685.
41 [9] A. Thayil K.N., A. Muriano, P. Salvador, R. Galve, M.P. Marco, D. Zalvidea, P. Loza-Alvarez, T.
42 Katchalski, E. Grinvald, A.A. Friesem, and S. Soria, Nonlinear immunofluorescent assay for androgenic
43 hormones based on grating waveguide structures, *Opt. Express*, 16 (2008) 13315-13322
44 [10] A. Muriano, A. Thayil K.N., P. Salvador, R. Galve, P. Loza-Alvarez, S. Soria and M.P. Marco, Two-
45 photon fluorescent immunosensor for androgenic hormones using resonant grating waveguide structures,
46 *Sens. Actuators B* 174 (2012) 394-401
47 [11] W. Denk, J.H. Strickler, and W. W. Webb, Two photon laser scanning fluorescence microscopy,
48 *Science* 248 (1990) 73-76.
49 [12] P. Schwille, U. Haupts, S. Maiti, and W.W. Webb, Molecular dynamics in living cells observed by
50 fluorescence spectroscopy with one and two photon excitation, *Biophys. J.* 77 (1999) 2251-2265.
51 [13] P.S. Dittrich and P. Schwille, Photobleaching and stabilization of fluorophores used for single
52 molecule analysis with one and two photon excitation, *Appl. Phys. B* 73 (2001) 829-837
53 [14] G. A. Cohoon, K. Khieu, and R.A. Norwood, Observation of two photon fluorescence of Rhodamine
54 6G in microbubble resonators, *Opt. Lett.* 39 (2014) 3098-3101.
55
56
57
58
59
60
61
62
63
64
65

1
2
3
4
5
6
7
8
9
10
11
12
13
14
15
16
17
18
19
20
21
22
23
24
25
26
27
28
29
30
31
32
33
34
35
36
37
38
39
40
41
42
43
44
45
46
47
48
49
50
51
52
53
54
55
56
57
58
59
60
61
62
63
64
65

[15] T. Carmon, L. Yang and K. Vahala, Dynamical thermal behavior and thermal self-stability of microcavities, *Opt. Express* 12 (2004) 4742-4750

[16] M. Brenci, R. Calzolari, F. Cosi, G. Nunzi Conti, S. Pelli and G. C. Righini, Microspherical resonators for biophotonic sensors, *Proceedings of SPIE* **6158** (2006). 61580S

[17] S. Berneschi, D. Farnesi, F. Cosi, G. Nunzi Conti, S. Pelli, G.C. Righini, and S. Soria, High Q microbubble resonators fabricated by arc discharge, *Opt. Lett.* **36** (2011) 3521-3522.

[18] L.L. Martin, P. Haro-Gonzalez, I. R. Martin, D. Navarro-Urrios, D. Alonso, C. Perez-Rodriguez, D. Jaque and N. E. Capuj, Whispering gallery modes in glass microspheres: optimizing of pumping in a modified confocal microscope, *Opt. Lett.* 36 (2011) 615-617

[19] F. Bestvater, E. Spiess ,G. Stobrawa, M. Hacker, T. Feurer, T. Porwol ,U. Berchner-Pfannschmidt ,C. Wotzlaw and H. Acker, Two-photon fluorescence absorption and emission spectra of dyes relevant for cell imaging, *J. Microsc.* 208 (2002)108-115

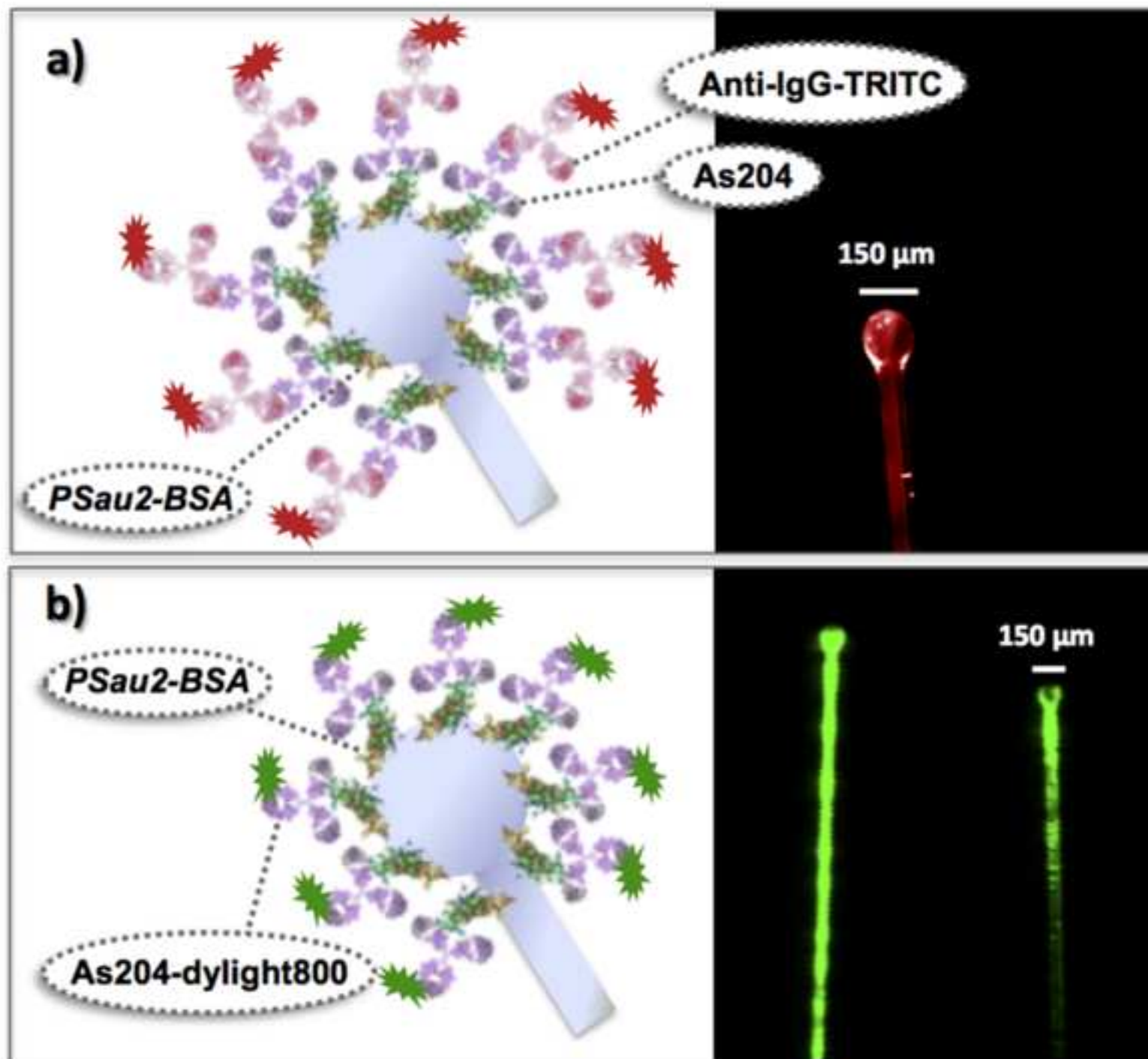


Figure
[Click here to download high resolution image](#)

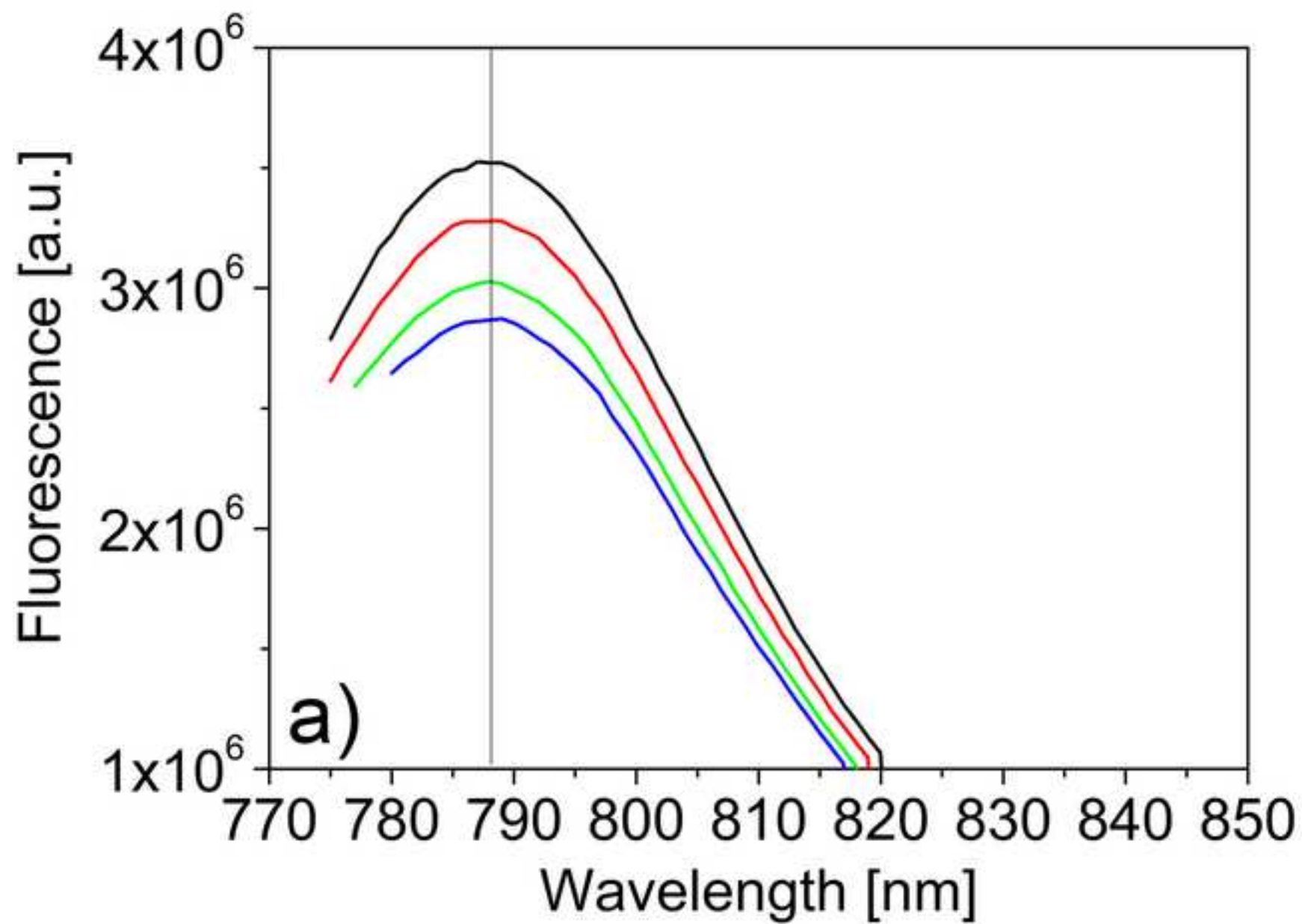


Figure
[Click here to download high resolution image](#)

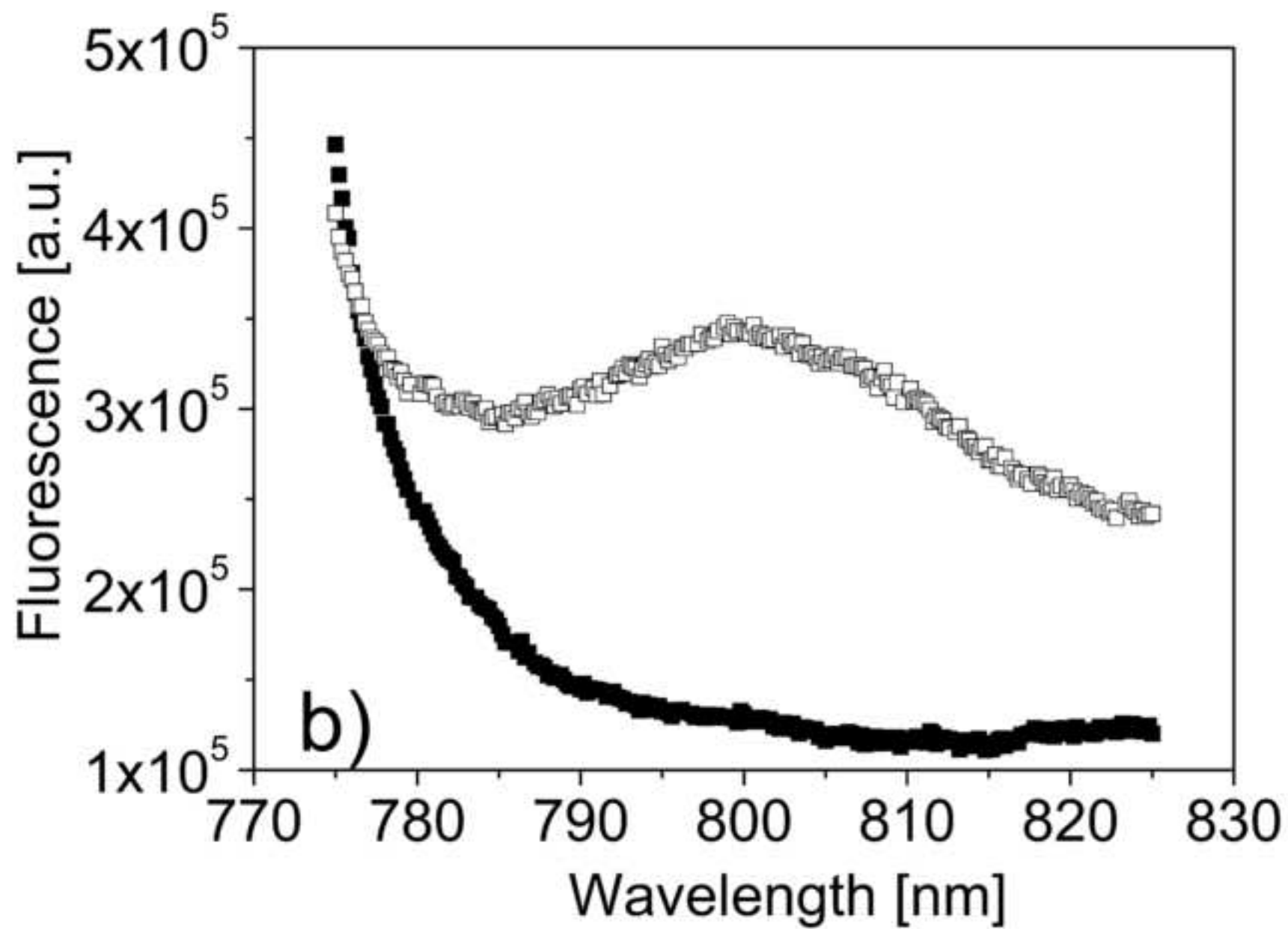
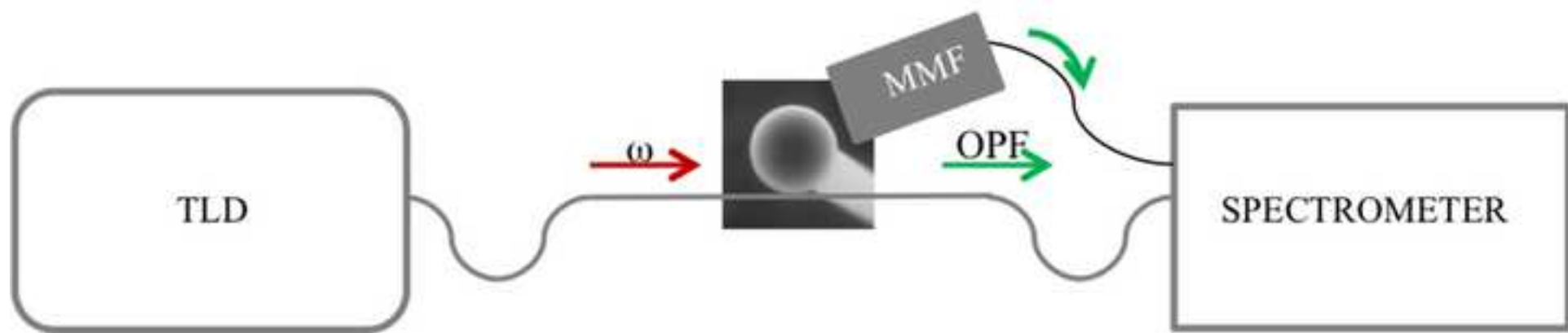


Figure
[Click here to download high resolution image](#)



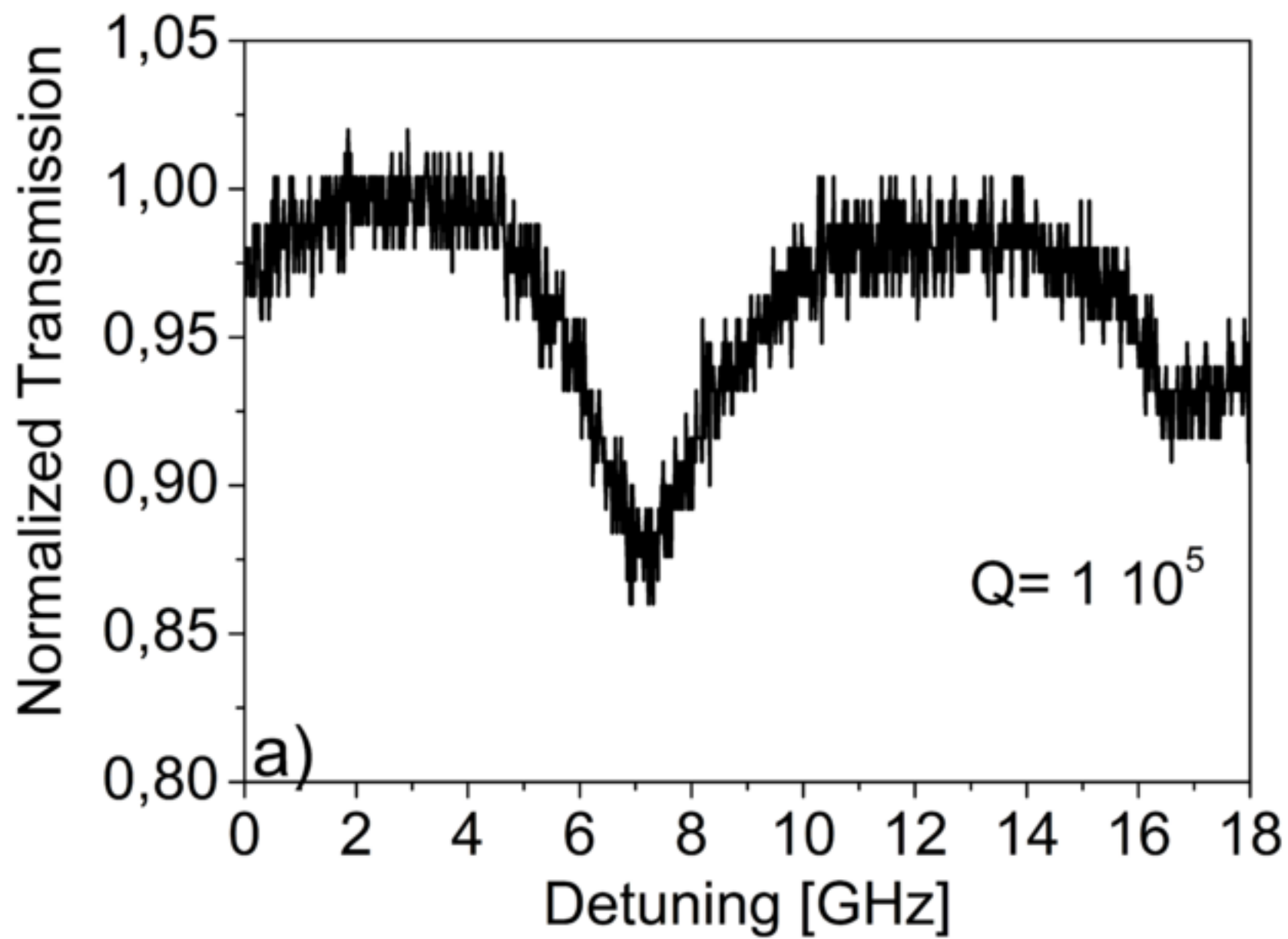


Figure
[Click here to download high resolution image](#)

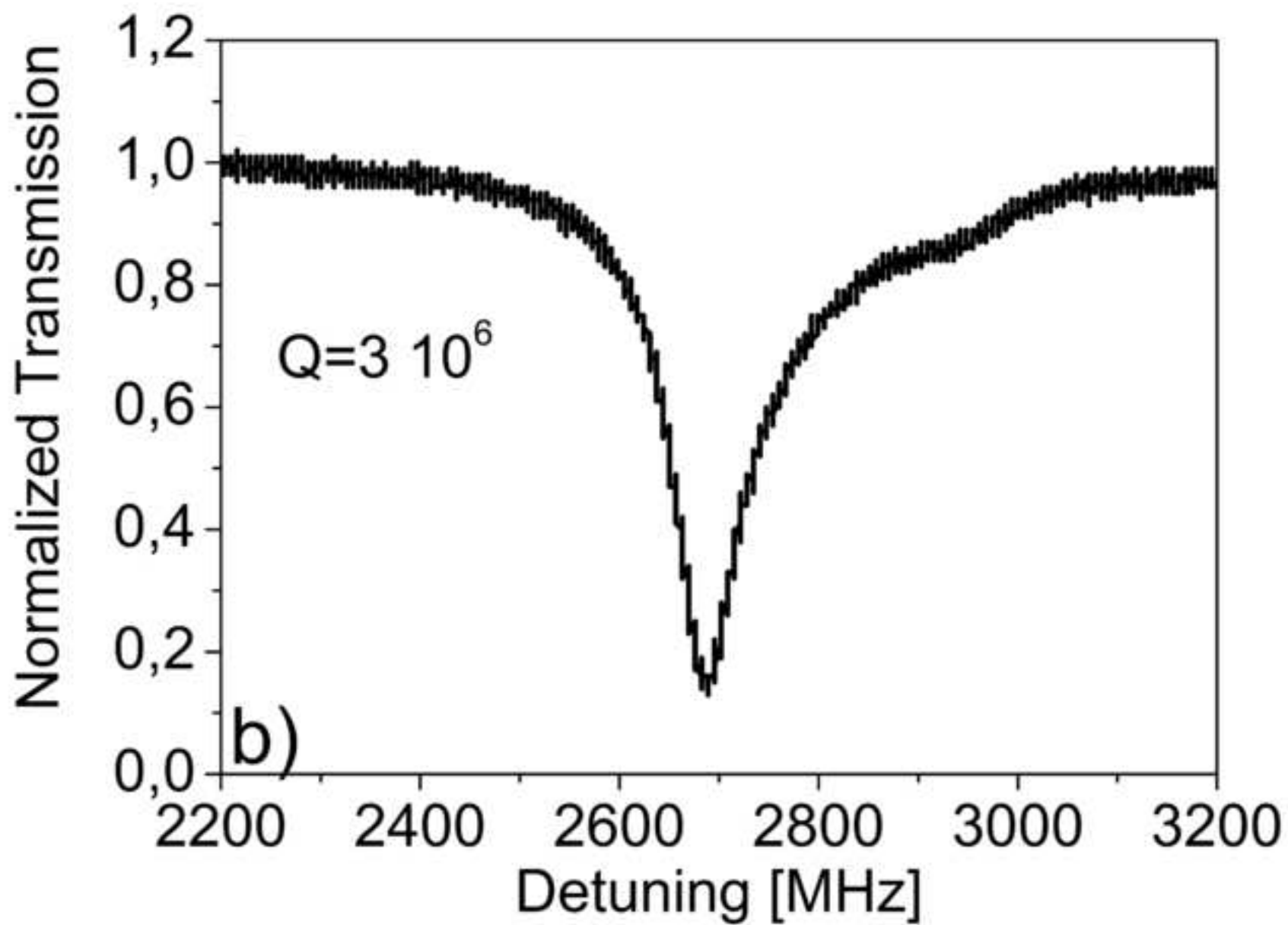
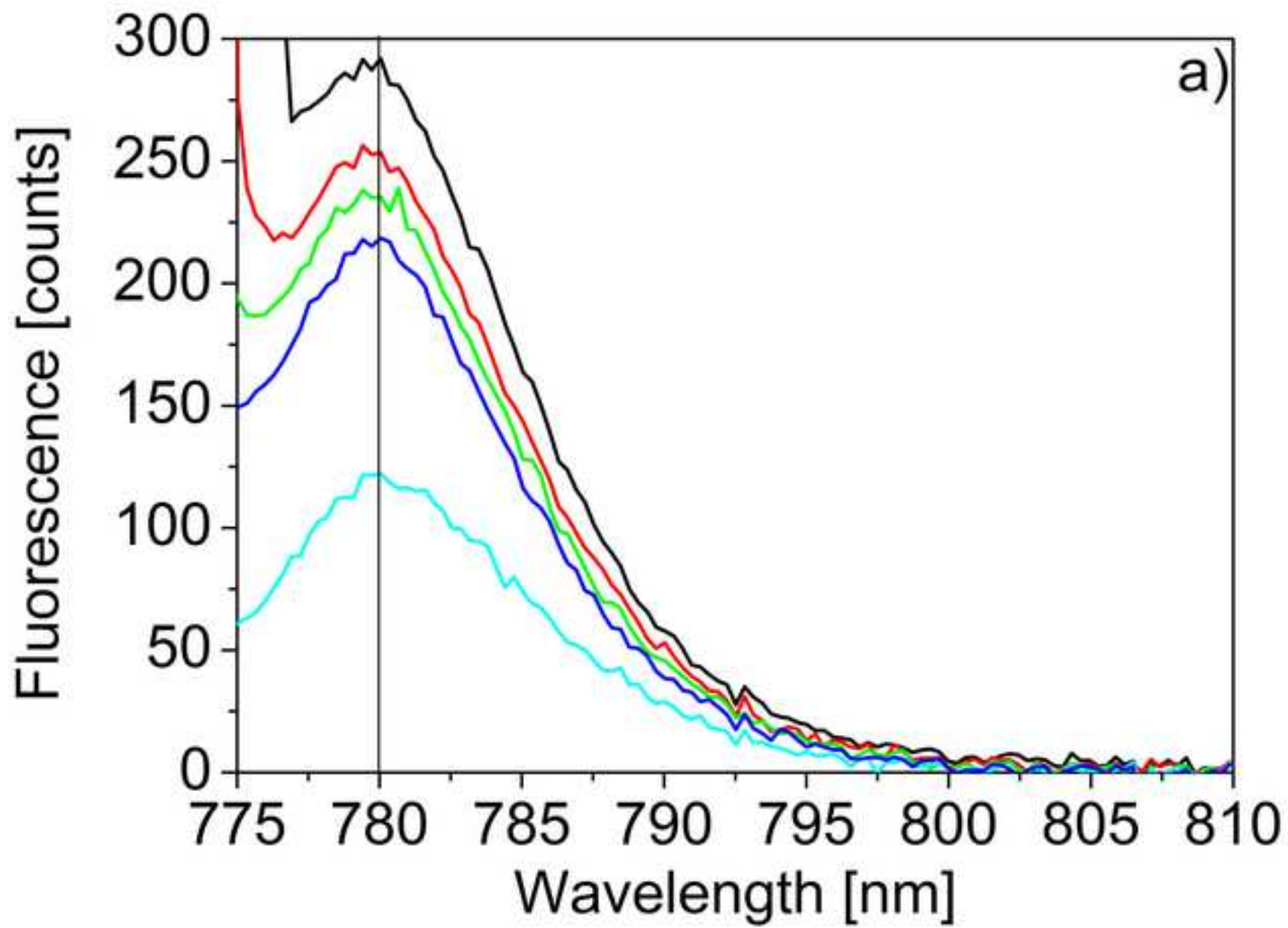
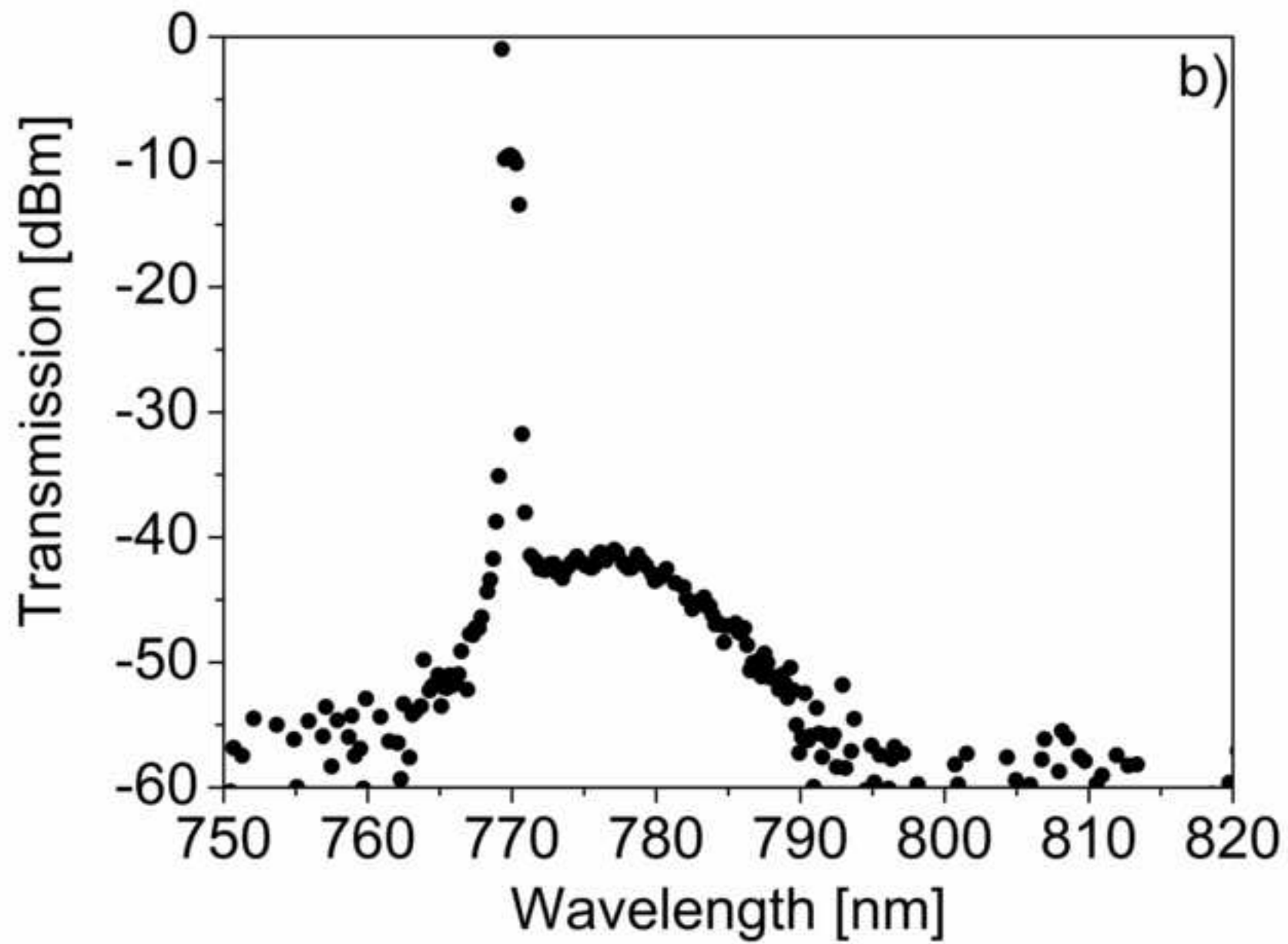


Figure
[Click here to download high resolution image](#)





Figure

[Click here to download high resolution image](#)



Figure

[Click here to download high resolution image](#)

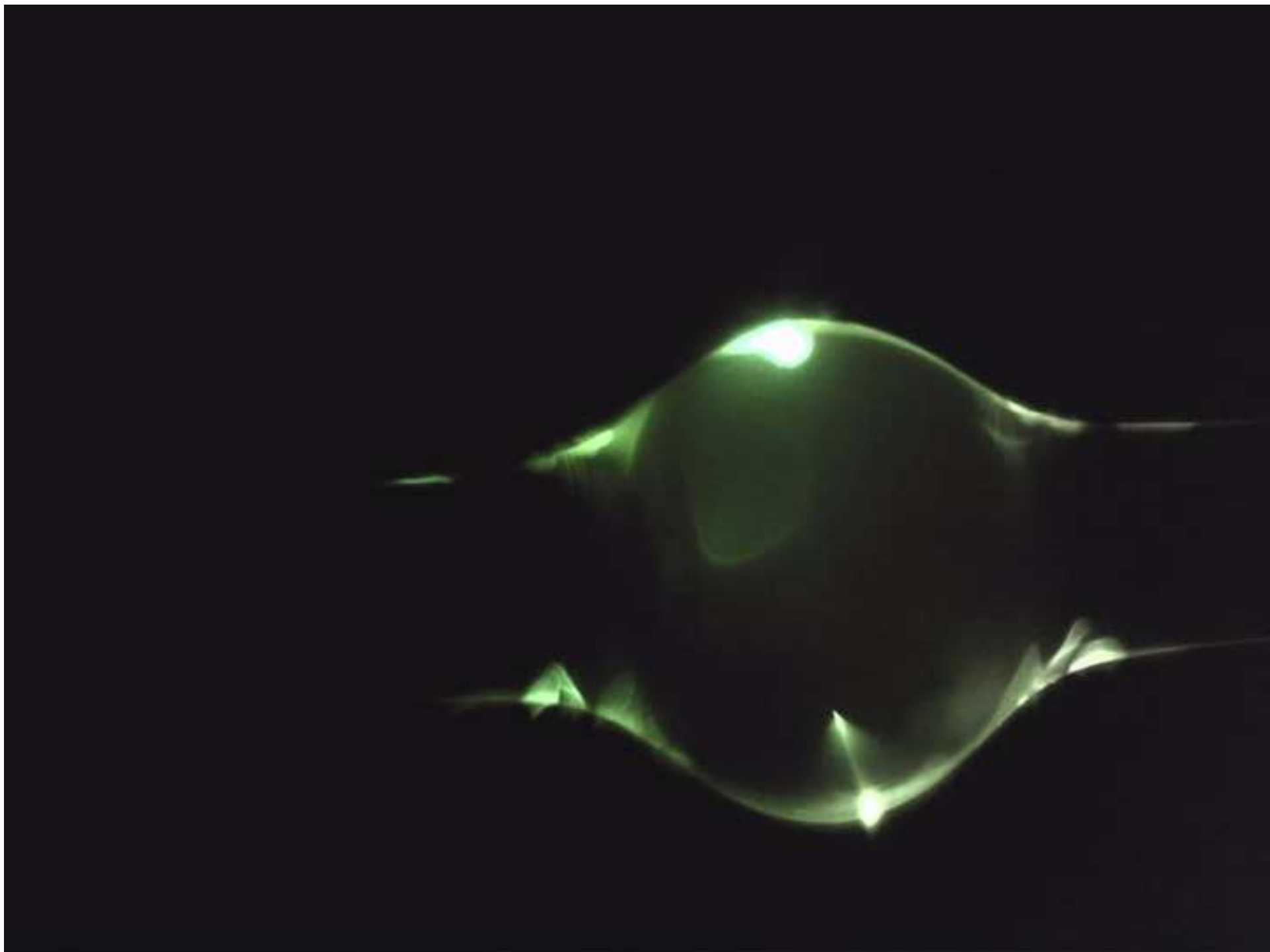
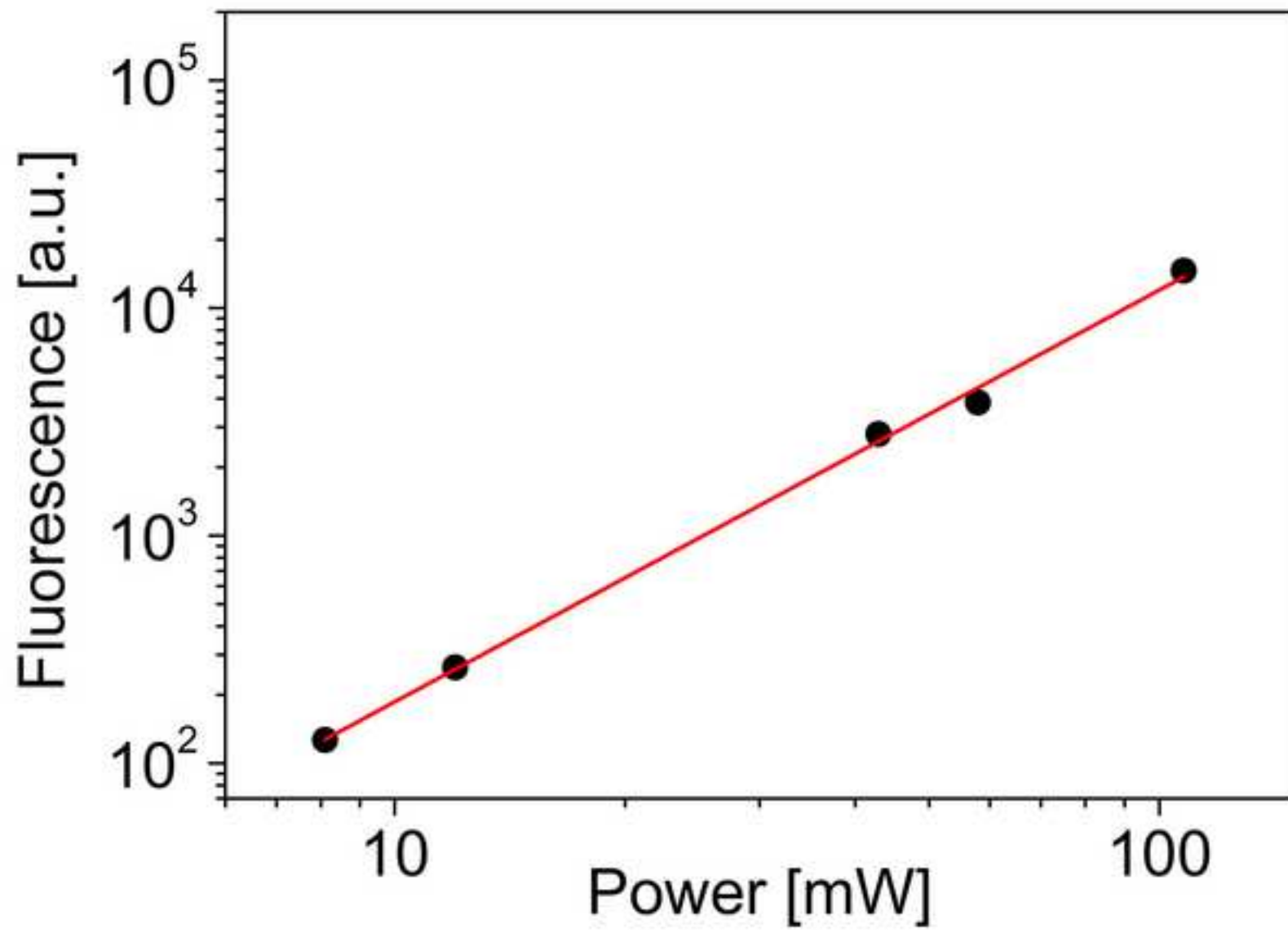


Figure
[Click here to download high resolution image](#)



Figure

[Click here to download high resolution image](#)

